Downscaling extreme short-term regional climate model precipitation for urban hydrological applications

Jonas Olsson, Ulrika Willén and Akira Kawamura

ABSTRACT

Urban hydrological climate change impact assessment requires an assessment of how short-term local precipitation extremes, e.g. expressed as intensity-duration-frequency (IDF) curves, are expected to change in the future. This cannot be done on the basis of regional climate model (RCM) results directly, mainly because of the models' coarse spatial grid and resolution-dependent limitations in process descriptions. In this paper, a stochastic model for downscaling short-term precipitation from RCM grid scale to local (i.e. point) scale is formulated and tested using data from Stockholm, Sweden. In principle, additional RCM variables characterising the weather situation are used to convert from grid box average to local precipitation, and estimate the probability of occurrence in an arbitrary point. Finally, local time series are stochastically simulated and IDF curves derived. The results of the application in Stockholm suggest that: (1) observed IDF-curves may be effectively reproduced by the model; and (2) the future increase of local-scale short-term precipitation extremes may be higher than the predicted increase of short-term extremes on the RCM grid scale.

Key words | climate change, intensity-duration-frequency curves, stochastic downscaling

Jonas Olsson (corresponding author)
Ulrika Willén
Research and Development,
Swedish Meteorological and Hydrological Institute,
Sweden
E-mail: *jonas.olsson@smhi.se*

Akira Kawamura
Department of Civil and Environmental Engineering,
Tokyo Metropolitan University,
Japan

INTRODUCTION

Urban hydrological modelling requires precipitation data at a very high resolution, in both time and space. In time, durations down to 5–10 min need to be considered. In space, generally observations from a single gauge (or a few gauges within a very limited area) are used. The precipitation input may be either continuous time series with observed historical sequences or idealised design storms. In the latter case, precipitation intensity is estimated from intensity-duration-frequency (IDF) curves (e.g. Chow *et al.* 1988).

The high resolutions required are problematic with respect to climate change assessment, as they are not matched by the resolutions used in global climate models (GCMs) and regional climate models (RCMs). The time steps commonly used for precipitation output in the latter (30 min, sometimes shorter) is rather close to the required temporal resolution, but the spatial grid is still relatively coarse (until now typically 50×50 km, but gradually getting finer) making direct RCM output unsuitable for direct application in urban hydrological climate change assessment (e.g. Semadeni-Davies *et al.* 2008; Olsson *et al.* 2009; Onof & Arnbjerg-Nielsen 2009).

The properties of short-term precipitation as observed in a single gauge and as averaged over a few thousand km^2, respectively, are very different (e.g. Chow *et al.* 1988). The most important difference concerns the extremes, as these are generated by different precipitation generating mechanisms. In Sweden, local short-term extremes are practically always generated in summer by localised convective events. However, on the scale representative of RCM grids, i.e. up to several 1,000 km^2, short-term extreme values are also caused by large-scale frontal events. Similarly, in terms of climate modelling, while the observed extremes can be very localised, a model grid box represents an average of surface types and heights. Thus, model extremes are expected to differ. Further, as the observed extremes occur over very short time periods, often shorter than the model time step, short-term atmospheric

doi: 10.2166/nh.2012.135

fluctuations will not be fully captured by the model. In these models, depending on the resolution and the convective parameterisation, localised convective events can occur either on the resolved model grid scale or on sub-grid scale. Thus, analyses of RCM extremes (and their changes) at the grid box scale may not reflect the properties of local extremes.

The objective of the study was to assess the possibility to statistically downscale extreme short-term (30 min) precipitation from the RCM grid scale to local scale. The main assumption behind the approach is that additional RCM variables characterising the current weather situation, mainly precipitation type and cloud cover, can be used to rescale grid box average precipitation to local precipitation. By assigning a probability that this local precipitation occurs in a specific point inside the grid box, realisations of point value time series may be stochastically generated. The overall idea is to formulate such a stochastic scheme, calibrate it to reproduce observed statistical properties for the present climate, and then apply the calibrated scheme to estimate future point precipitation statistics.

STUDY AREA AND DATA

The study focuses on Stockholm, the largest city in Sweden. Especially in the central parts of the city, the sewer system is old and already today its capacity is sometimes exceeded during heavy rainfall events. Future changes in the short-term precipitation extremes may thus have a strong impact on the system performance and flood risk.

Local precipitation observations

Daily precipitation volumes (resolution 0.1 mm) during the period 1980–2007 were extracted from the Stockholm station in the national network of the Swedish Meteorological and Hydrological Institute, located at the Royal Institute of Technology campus in the northern part of central Stockholm.

In urban hydrology and design, the properties of short-term rainfall extremes are generally compactly described in the form of IDF curves, based on extracted rainfall maxima for different durations. In engineering practice, IDF curves are used to determine which rainfall intensity a storm water sewer must be able to handle. In Swedish guidelines, sewer system design is commonly based on a rainfall with a 10-year return period and a duration of 1 h, although the latter depends on the catchment size (Svenskt Vatten 2004).

Hernebring (2006) carried out IDF analyses of short-term data from 15 stations all over Sweden, including 20 years of tipping-bucket observations from a gauge in Stockholm. Hernebring (2006) proposed the following general relationship (IDF curve)

$$I = e^{(k_{11}+k_{31}/D)} * R^{(k_{12}+k_{32}/D)} * D^{(k_{21}+k_{22}*\ln(R))} \quad (1)$$

where I denotes intensity, D duration, R return period and k location-specific constants. The relationship was found valid between durations of 5 min and 24 h. For Stockholm the constants were found to be $k_{11} = 6.24$, $k_{12} = 0.53$, $k_{21} = -0.69$, $k_{22} = -0.031$, $k_{31} = -1.77$ and $k_{32} = -0.61$. Hernebring (2006) does not show the agreement between observed intensities and the fit of Equation (1) for Stockholm, but in total, over all stations considered, the fit appears very accurate.

Climate model simulations

The climate model data used are extracted from simulations with the RCM RCA3. Below, its cloud and precipitation parameterisations are outlined and the extracted data described. For a full model description, see Jones *et al.* (2004) and Kjellström *et al.* (2005).

Clouds and precipitation in climate models are difficult to predict as most clouds are produced by condensation processes that take place on spatial scales much smaller than the size of a model grid box, e.g. clouds produced by cumulus convection, boundary layer turbulence, gravity waves or orographic lifting. These clouds have to be parameterised as functions of the prognostic variables explicitly resolved by the model, without losing the information about the physical processes that occur on the sub-grid scale and that are responsible for these clouds (Bony & Emanuel 2001). Cloud fraction parameterisations can be classified into two main types, diagnostic schemes and statistical schemes. The statistical schemes use specified probability distribution

functions (PDFs) to represent sub-grid scale variability of total water (water vapour, cloud water and ice). The cloud fraction can be determined from the supersaturated part of the PDF. The shape and width of the distributions are determined from observations or high resolution cloud resolving models.

RCA3 cloud parameterisation belongs to the diagnostic group and has cloud processes separated into resolved (large- and meso-scale) clouds (described according to Rasch & Kristjánsson 1998), and sub-grid scale (convective) clouds (Kain & Fritsch 1990). The diagnosis of the cloud fraction in a grid square follows the ideas of Slingo (1987). Precipitation is calculated for the resolved and sub-grid scale clouds separately. In this report we will refer to them as large scale and convective precipitation, bearing in mind that the RCA3 resolved precipitation also contains convective parts. Brown (1979) estimates that up to 40% of the precipitation reaching the ground in a typical convective system originates from the meso-scale cloud system

The data used here are results for Stockholm extracted from four RCA3 simulations. The first is a simulation from 1980 to 2007 using meteorological reanalyses as boundary fields; ERA40 from 1980 to mid-2002 and operational ECMWF analyses from mid-2002 to 2007 (we hereafter refer to this simulation as ERA). This simulation represents RCA3 performance under ideal conditions, as the boundary is based on observations, and is therefore the most suitable for comparison with observations.

For estimation of future changes, RCA3 results were extracted from simulations with GCM boundary fields; two transient ECHAM4-projections (IPCC scenarios A2 and B2) and one ECHAM5-projection (A1B) (hereafter referred to as A2, B2 and A1B, respectively). No other projections with the required time resolution were available for this study. The transient runs cover the entire period from 1961 to 2100, but four 30-year periods have been defined for this study: 1971–2000 (reference period; REF), 2011–2040 (future climate 1; FC1), 2041–2070 (FC2) and 2071–2100 (FC3). All runs were performed over Europe at 50 km horizontal resolution with a 102×111 grid and 24 vertical levels.

As the investigation is focused on Stockholm, time series of precipitation and cloud variables from five grid boxes, each thus representing an area of 50×50 km, in the region have been extracted and analysed; one centred over central Stockholm and the one in each quarter (N, E, S, W). The extracted variables are:

- total precipitation, TP (time step: 30 min)
- large and meso-scale precipitation (resolved), LP (3 h)
- convective precipitation (sub-grid scale), CP (3 h)
- total cloud cover: total, TC (3 h)
- high clouds, HC (6 h).

For all variables the time resolution is the highest available. The total cloud cover as viewed from the surface is in RCA3, calculated assuming maximum-random overlap, which is supported by observations (e.g. Willén *et al.* 2005). This means that adjacent cloud fractions in the vertical column (e.g. convective tower cloud extending over several model levels) are vertically stacked, i.e. in maximum overlap, while if the cloud fractions are separated by clear air (e.g. a cirrus cloud above low level shallow cumulus) they are assumed to be in random overlap. High clouds in RCA3 are defined as the maximum cloud fraction above 450 hPa, medium clouds (the maximum cloud fraction in the pressure range 800 to 450 hPa) and low clouds (the maximum cloud fraction below 800 hPa).

DOWNSCALING METHODOLOGY

The principle of the suggested downscaling approach is shown in Figure 1. In the RCM output, total grid box average precipitation P consists of one resolved (large-scale) component and/or one convective component, P_f and P_c in Figure 1 (P_f corresponds to LP above and P_c to CP). Each of these is assumed to be associated with a cloud cover fraction, C_f and C_c ($0 \leq C \leq 1$), respectively, represented by the white area in Figure 1. It is further assumed that the cloud cover fraction C is related to the fractional precipitation area A (A_f and A_c; shaded area in Figure 1) by a multiplicative parameter α, $0 < \alpha \leq 1$. Under these assumptions the actual local precipitation P_{point}, which occurs in a point located under the precipitation field, is given by P/A. If further assuming that the probability of precipitation is the same everywhere inside the grid box, the probability of P_{point} occurring in an arbitrary point inside the grid box equals the fractional precipitation area A.

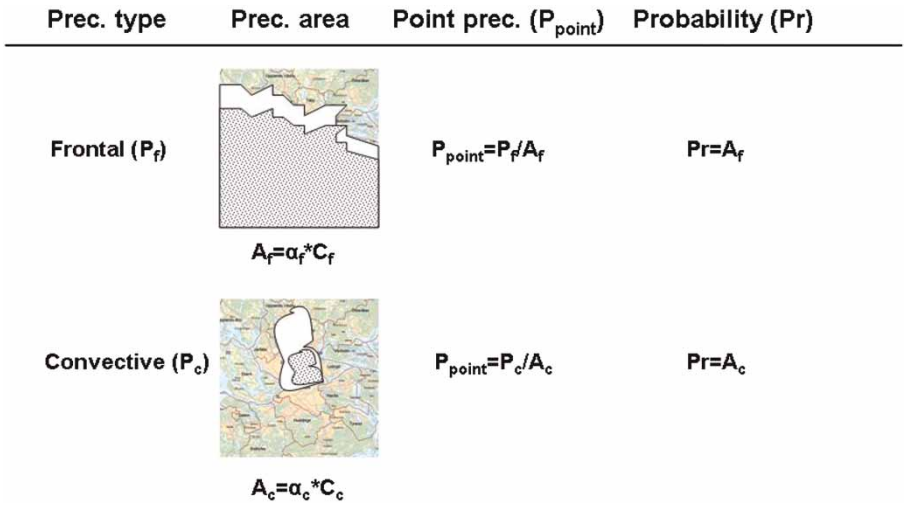

Figure 1 | Schematic of the stochastic downscaling scheme.

Under these assumptions stated, a simplified scheme for stochastic simulation of precipitation time series in an arbitrarily located gauge may be developed. For each time step, the procedure is as follows:

- rescale the grid box average precipitation to a local precipitation P_{point} mm based on the fractional cloud cover C and the associated precipitation area A;
- generate a uniformly distributed random number r ($0 < r < 1$);
- if $r > A$ the precipitation field misses the gauge which thus registers 0 mm;
- if $r < A$ the precipitation field hits the gauge which registers P_{point} mm.

By repeating the procedure for all time steps, a continuous local short-term precipitation time series may be generated.

As the precipitation downscaling scheme is stochastic, each time it is applied (with a new seed) to the same grid box time series a different point time series realisation is generated. The downscaling results presented in the following represent averages over 100 realisations, which were found to be sufficient for obtaining stable estimates. Downscaling was attempted both with and without tuning the estimation of the rainfall area A based on the cloud cover C. No tuning implies that the multiplicative parameter $\alpha = 1$, i.e. the precipitation area A equals the cloud cover C.

RESULTS AND DISCUSSION

Before model evaluation and application, an evaluation of the climate model data is carried out to assess their realism and applicability for the present purpose. Model evaluation is then performed using the ERA simulation, after which the model is applied to downscale the future climate projections (A2, B2, A1B).

Evaluation of climate model data

From visual inspection, the annual cycle of total precipitation in the ERA simulation is in good agreement with that of the SMHI gauge, with least precipitation in spring and most in summer (Figure 2). The large-scale fraction is relatively stable in winter, spring and summer, but significantly higher in autumn. This is possibly a reflection of higher frequency of cyclones in this season. The contribution from active convection is significant only in summer when the land surface gets unevenly heated and nimbostratus clouds of large vertical extent can build up resulting in large precipitation amounts.

An IDF analysis was performed for the ERA time series and the resulting curves were averaged over the five grid boxes considered. For the return period of 15 years and duration 30 min, the difference between the observed and simulated intensity corresponds to a factor of 10 (Figure 3(a)).

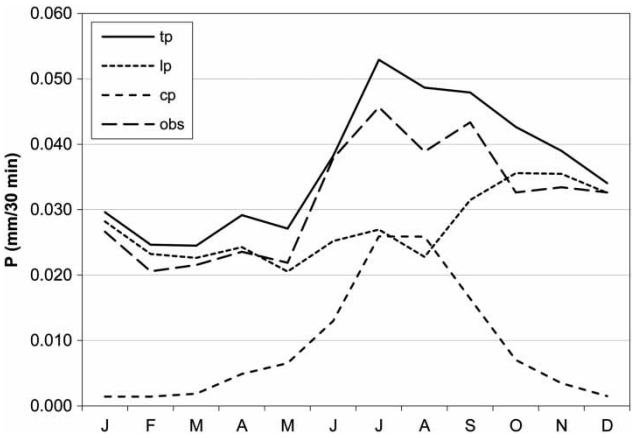

Figure 2 | Annual cycles (1980–2007) of total (tp), large-scale (lp) and convective (cp) precipitation amounts in the ERA simulation and in the SMHI gauge (OBS) in the period.

Moving towards longer durations, however, the difference decreases and at 1 day the curves nearly converge. Convergence means that the point precipitation and the spatially averaged precipitation are identical, i.e. approximately the same precipitation falls everywhere inside the grid box. This in turn implies that the rainfall field produced by the type of synoptic or convective systems that generate 1-day extremes are of at least the same spatial extension as the model grid boxes. On the other hand, the rainfall systems generating short-term (sub-hourly) point extremes are mainly localised convective systems too small to produce significant spatial averages.

The curves representing shorter return periods are in principle similar to the 15-year curve (Figure 3(b–d)). However, whereas the observed intensities substantially decrease with decreasing return period, the simulated intensities decrease only slightly. Thus the highest spatially averaged ERA intensities are rather similar, whereas the observed point precipitation extremes are more variable.

One aspect of the differences is the impact of spatial averaging and the resulting difference between gridded data with single point observations. Several attempts to estimate areal reduction factors (ARFs) describing the impact of spatial averaging have been made. In NERC (1975), the recommended ARF for a 30 min rainfall in UK extending over 3,000 km^2 is ~0.4 (with no dependence on return period). A point 30 min intensity of 50 mm/h would thus correspond to ~20 mm/h for an area of the size of the RCA3 grid, which is still ~4 times higher than the actual RCA3 value obtained (Figure 3(a)). As the return period decreases, however, the RCA3 value becomes gradually closer to a value of 0.4 times the observed value (Figure 3(b–d)). Although admittedly a very crude assessment, this may be taken as a weak indication that RCA3 underestimates short-term precipitation extremes, to an increasing degree with increasing return period. The recommended ARF for a 1-day rainfall over 3,000 km^2 is ~0.85 (NERC 1975), which is close to the ratio between observed and RCA3-derived curves for return periods 3 years and 1 year (Figure 3(c–d)).

Another aspect concerns limitations in the climate model. We expect the model extremes to be less than the observed extremes due to the limited spatial and time resolution, mismatch in time and space (the model dynamical systems might be slightly shifted which has a large impact on the specific location) and due to shortcomings of the parameterisations. Heavy rainfall events are largely affected by the local scale and therefore we do not expect a model at 50 km (or even 10 km) resolution to capture the highest events. The model surface and orography characteristics are smoother and can differ substantially from the values at a measuring site. Furthermore, the most intense observed values occur at time intervals shorter than 30 min, whereas the model can only resolve atmospheric phenomena on time scales larger than the model time step, which is 30 min.

An evaluation of the RCA3 cloud variables has been performed by Willén (2008) with a comparison with satellite observations. The analysis covered Europe entirely, but for this paper results have been extracted for the Stockholm region. A visual comparison between simulated and observed cloud cover on a monthly basis in the period of 1997–2001 indicates that, overall, the simulated cloud cover effectively reproduces the observed one (Figure 4).

Model evaluation for present climate

The IDF-curves of point precipitation downscaled by the stochastic scheme without tuning are substantially closer to the observed curves than the IDF-curves produced from RCA3 grid box data, especially for the shortest durations (Figure 5(a–b)). The observed values are, however, still notably higher, i.e. the downscaled extreme intensities are underestimated. At long durations the downscaling

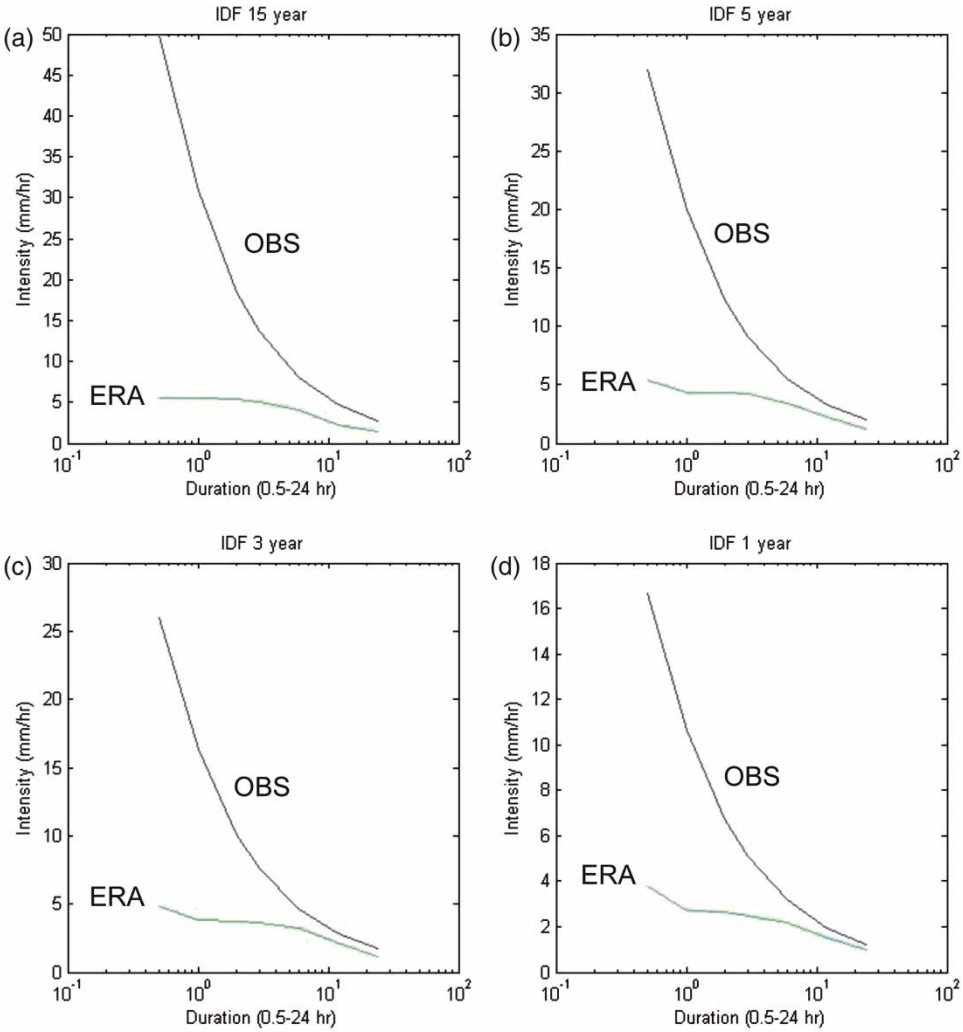

Figure 3 | IDF curves representing observations (Equation (1); OBS) and ERA simulation grid box output (ERA) for return periods 15 (a), 5 (b), 3 (c) and 1 (d) year(s). Note that different scales are used on the y-axis.

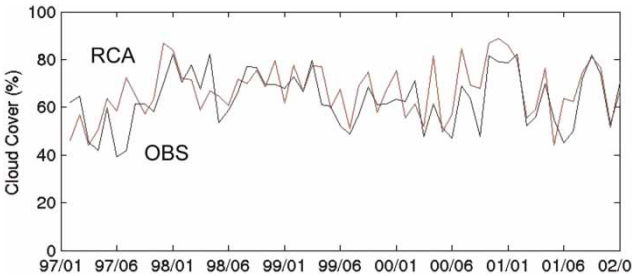

Figure 4 | Monthly total cloud cover in Stockholm as observed (OBS) and as simulated by RCA3 (RCA).

has no effect. This is generally because these extremes are generated by large-scale synoptic systems with cloud cover C equal or close to 1, i.e. point precipitation becomes equal or close to the grid box average precipitation.

Attempts to improve the agreement between observed and downscaled IDF-curves were made by calibration of the α-parameter to an optimal value below 1. This means that the generated rainfall field is smaller than the cloud cover, which is physically reasonable.

For the ERA-simulation, an α_c-value of ~0.12 was found to be optimal. In some cases, however, when HC is small, this makes A_c very small and then P_{point} may become unrealistically high. Therefore, a minimum HC-threshold was used. A value ~0.1 (i.e. 10% fractional cover) was found suitable. With a grid size of 50×50 km and an α_c-value of 0.12, a

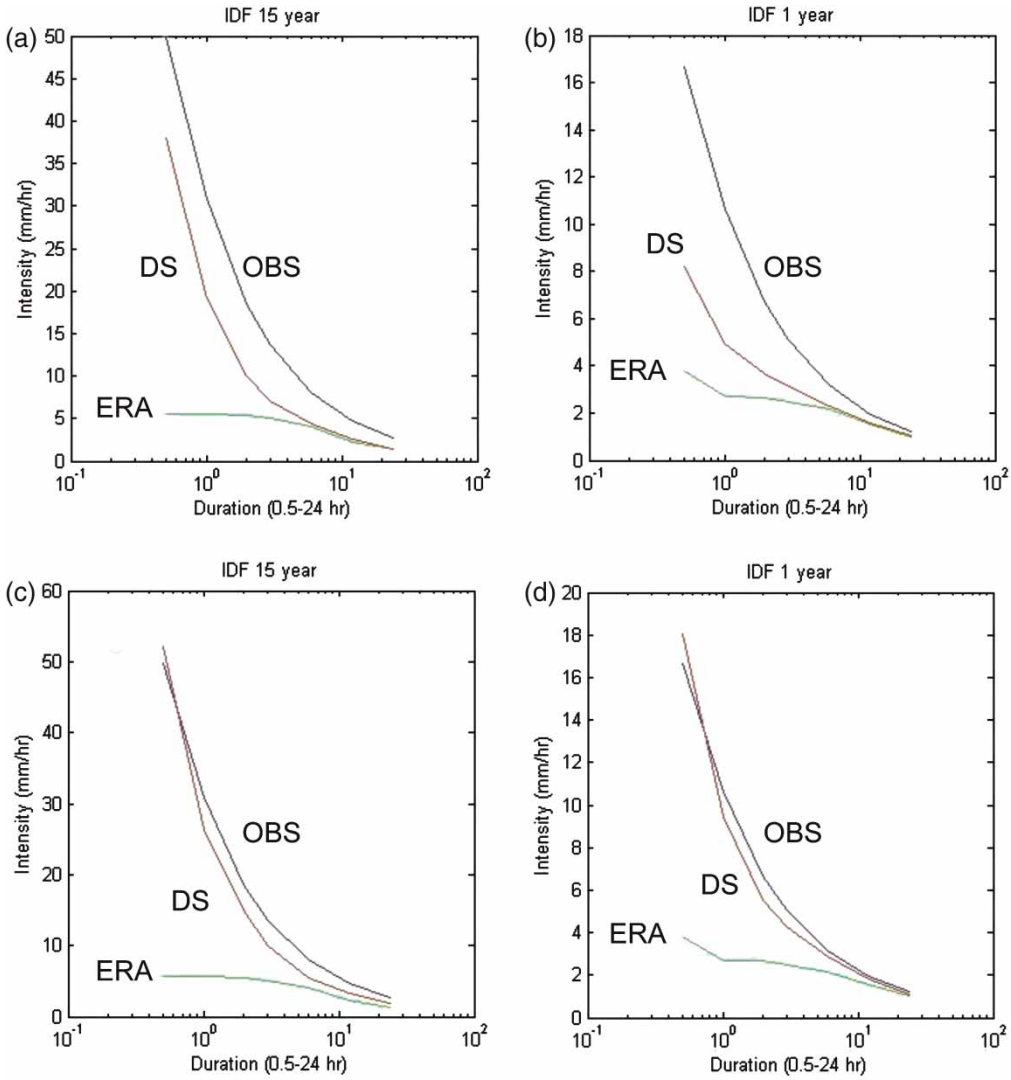

Figure 5 | IDF curves representing observations (Equation (1); OBS), ERA simulation grid box precipitation (ERA) and point simulations by downscaling (DS). Top row: untuned downscaling for return periods 15 years (a) and 1 year (b). Bottom row: tuned downscaling for return periods 15 years (c) and 1 year (d).

threshold of 0.1 implies that 30 km^2 would be a lower limit of the spatial extension of the 30 min areal rainfall generated by convective precipitation. Further work will aim at verifying this value on theoretical and/or empirical grounds.

Concerning frontal precipitation, instead of reducing the area of TC by the parameter α_f, it was found more suitable to use a cut-off limit for the large-scale precipitation component P_f. This change is also done in other hydrological applications of the RCA3 (and other GCM/RCM) data, to remove excessive and possibly spurious low precipitation. In this application a threshold of ~0.15 mm was found optimal. It may be noted that the treatment of large-scale precipitation has only a minor impact on the simulated IDF-curves which are governed by convective precipitation.

From visual inspection, the results indicate that it is possible to effectively reproduce the observed IDF-curves by tuned downscaling (Figure 5(c–d)). The main difference between the observed and downscaled curves is a somewhat higher degree of curvature in the simulated curves, i.e. the rate of increase in extreme intensity with decreasing

duration is somewhat overestimated. It does, however, not seem possible to significantly change the curvature by the present simple formulation of the downscaling scheme.

Model application for future climate

The stochastic downscaling scheme was applied to the A2, B2 and A1B projections, using both untuned and tuned downscaling. In the latter, the parameters were optimised to fit the observed IDF curves using data in the REF period 1971–2000 (the same parameter values were used for all projections). The resulting parameter values were similar overall to those obtained in the optimisation to RCA3/ERA40 data described above.

The resulting 10-year IDF-curves indicate a future increase in the short-term point precipitation extremes (Figure 6). In the B2 projection, most of the increase occurs between REF and FC1, with a rather minor additional increase until FC3. In the A1B projection, however, most of the increase occurs between FC1 and FC2, and in A2 the increase from REF to FC3 is gradual (not shown).

Relative changes in 10-year precipitation intensity of different durations, i.e. effectively the ratios of future to present IDF-curves, were calculated (Figure 7). Looking first at tuned downscaling and FC1 (Figure 7(a)), there is a substantial variation between the projections. In B2 the short-duration extremes increase by some 20% whereas the long-duration extremes decrease by almost the same amount. This implies an increased intensity of localised, convective rainfalls, but a decreased intensity of precipitation associated with large-scale synoptic systems. In A1B the picture is almost the opposite, with a small decrease of short-duration extremes and a 20–30% increase of the long-duration extremes. The change found in projection A2 is in between the others. On average, over all projections the change ranges from 10% for a duration of 30 min to 3% for a duration for 1 day.

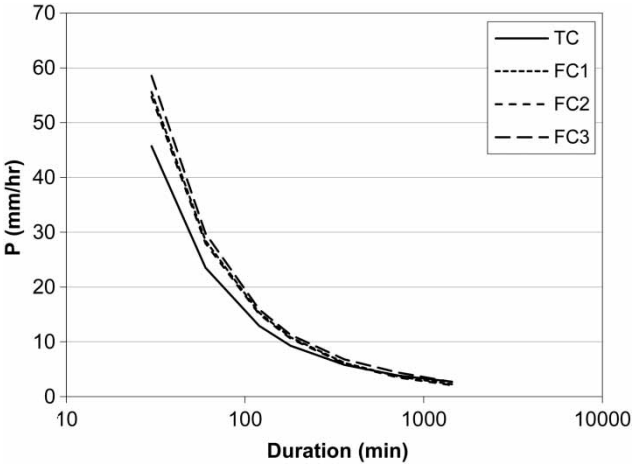

Figure 6 | 10-year IDF-curves for the 30-year periods (REF: 1971–2000; FC1: 2011–2040; FC2: 2041–2070; FC3: 2071–2100) estimated by tuned downscaling (projection B2).

The changes obtained for period FC3 vary similarly to the ones found for FC1, but are consistently shifted upwards by some 10% (Figure 7(b)). The average change ranges from 20% for 30 min to 13% for 1 day.

The changes estimated from untuned downscaling (Figure 7(c–d)) are similar overall to the ones from tuned downscaling, with similar trends in the projections and similar levels of the average changes. One difference is that the rather clear tendency of a larger increase for shorter durations found is not evident in the untuned downscaling. A possible explanation is that the future increase of short-term convective extremes becomes accentuated in the tuned downscaling, because of its stronger concentration of grid box precipitation into smaller areas.

Finally, the future changes in short-term point precipitation extremes estimated using downscaled time series are compared with the changes estimated directly from RCA3 grid box average precipitation time series (Figure 8). For FC1, a small average decrease by 4% of the short-term extremes at the grid scale is suggested (Figure 8(a)). As the changes in individual projections vary widely by ±20% over the entire range of projections, effectively no difference from REF is found. For FC3, the average grid scale change ranges from 15% for 30 min to 8% for 1 day (Figure 8(b)). In this case there is much less variation between the projections but they are all rather close to the average curve.

The relative increase estimated from downscaled series is consistently 5–10% larger than that estimated from the grid box series (Figure 8). This finding may indicate that the future increase in local short-term point precipitation extremes, which are mainly related to convective events, becomes larger than the short-term increase estimated from 50 km RCA3 grid box average precipitation, which is mainly related to large-scale events. However, it must be

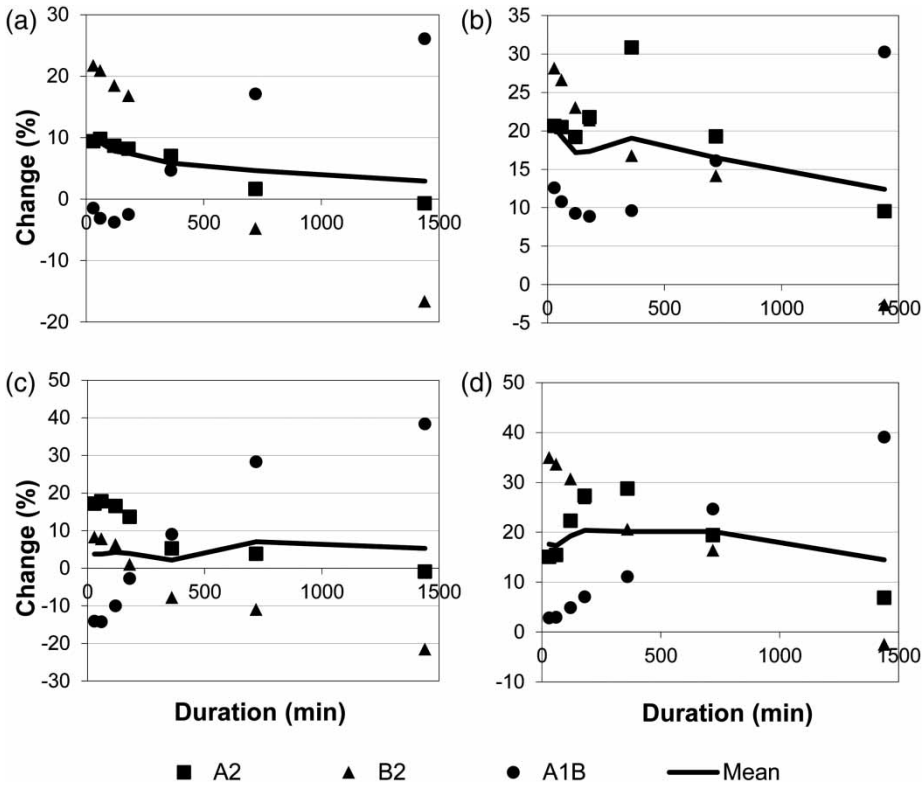

Figure 7 | Relative changes in 10-year precipitation intensity in projections A2, B2 and A1B (black circles) and mean changes (lines). Top row: tuned downscaling for period FC1 (2011–2040; (a)) and FC3 (2071–2100; (b)). Bottom row: untuned downscaling for period FC1 (c) and FC3 (d).

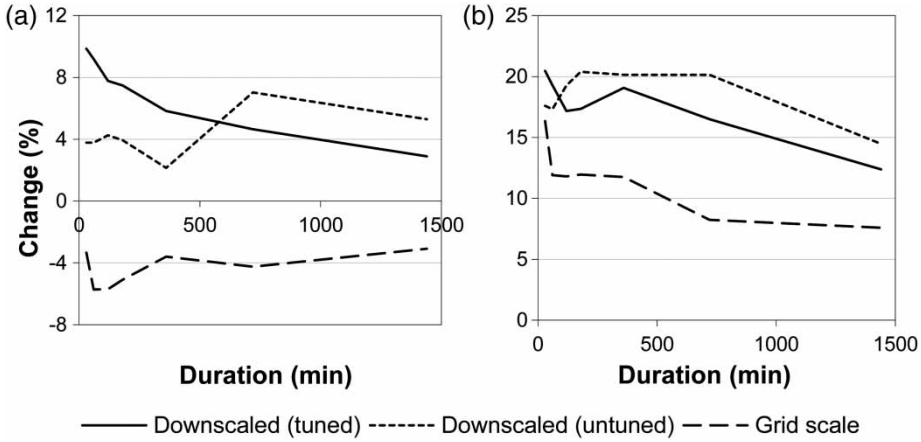

Figure 8 | Relative change in 10-year precipitation intensity from REF to FC1 (2011–2040; (a)) and FC3 (2071–2100; (b)) estimated by tuned downscaling, untuned downscaling and at the grid box scale. The curves represent averages over the three projections used, i.e. A2, B2 and A1B.

emphasised that the application of the stochastic downscaling scheme to the original RCA3 grid box data introduces a substantial amount of uncertainty. Thus, while supposedly better representing local precipitation, the changes estimated from downscaled series are clearly less robust than the changes at grid box scale. A practical approach may be to view the grid scale changes as conservative estimates of changes also on smaller scales.

CONCLUSIONS

- The annual cycle of mean monthly total precipitation from RCA3 agrees well with observations, although a slight overestimation is found. However, the frequency is overestimated, especially of large-scale (resolved) precipitation. Also, the mean monthly RCA3 cloud cover agrees well with observations.
- After tuning, a simple stochastic downscaling scheme based on precipitation type and cloud cover can simulate point precipitation time series which effectively reproduce observed extreme statistics.
- The downscaled series indicate a 5–10% increase in short-term extreme intensities in the period 2011–2040 and a 10–20% increase in the period 2071–2100. This is 5–10% more than estimated from RCA3 grid box data.

The main finding is the indication of a larger increase in future short-term extreme precipitation on the point scale than on the RCM RCA3 grid scale. Thus, the future increase of local precipitation intensities may become larger than inferred from direct climate model output. However, as the downscaling involves precipitation and cloud variables associated with high uncertainty, the point scale results must be considered less robust than the grid scale results and thus the results must be interpreted with caution.

It must be emphasised that the suggested downscaling scheme is mainly intended as a prototype to be further developed. For example, other RCM variables than the ones used here may be better predictors for estimating the fractional precipitation area. Further, besides the extreme statistics assessed here, preliminary evaluation has indicated that the downscaled time series overall also effectively reproduce the most relevant average statistical properties in the observations, e.g. annual total, wet fraction and the volume and duration of individual precipitation events. Because the adjacent time steps are independent, however, the autocorrelation in downscaled point time series becomes lower than in observed series. Including temporal correlation is thus another potential development.

It must also be emphasised that this is a case study for a specific location and a specific set of climate projections. To assess the general applicability of the approach, further tests in other locations using other observations and a larger ensemble of climate projections are ongoing. A key issue is the current rapid increase in the spatial resolution of RCMs, which is approaching 10 km^2 and even higher. At this resolution, grid scale model precipitation is potentially far better at representing point precipitation than at today's typical RCM resolutions ($\geq 25 \times 25$ km) Thus, besides developing tools for downscaling, evaluation of high-resolution RCM precipitation is an important future task.

ACKNOWLEDGEMENTS

The study was mainly performed within the project Mistra-SWECIA, funded by the Foundation for Strategic Environmental Research (MISTRA). Funding was also provided by the Swedish Research Council Formas, through project Hydroimpacts 2.0, and by Tokyo Metropolitan University. We gratefully acknowledge this funding. We also thank two reviewers for helpful comments on the original manuscript as well as Erik Kjellström and Anders Ullerstig for providing most of the RCA3 data used in this study.

REFERENCES

Bony, S. & Emanuel, K. A. 2001 A parameterization of the cloudiness associated with cumulus convection; Evaluation using TOGA COARE data. *J. Atmos. Sci.* **58**, 3158–3183.

Brown, J. M. 1979 Mesoscale unsaturated downdrafts driven by rainfall evaporation. *J. Atmos. Sci.* **36**, 313–38.

Chow, V. T., Maidment, D. R. & Mays, L. W. 1988 *Applied Hydrology*. McGraw-Hill, Inc., USA.

Hernebring, C. 2006 *Design Storms in Sweden Then and Now*. VA-forsk publ. 2006–04, Svenskt Vatten, Stockholm (in Swedish).

Jones, C. G., Ullerstig, A., Willén, U. & Hansson, U. 2004 The Rossby Centre regional atmospheric climate model (RCA). Part I: Model climatology and performance characteristics for present climate over Europe. *Ambio* **33**, 199–210.

Kain, J. S. & Fritsch, J. M. 1990 A one-dimensional entraining/detraining plume model and its application in convective parameterization. *J. Atmos. Sci.* **47**, 2784–2802.

Kjellström, E., Bärring, L., Gollvik, S., Hansson, U., Jones, C., Samuelsson, P., Rummukainen, M., Ullerstig, A., Willén, U. & Wyser, K. 2005 *A 140-year simulation of the European Climate with the new version of the Rossby Centre Regional Atmospheric Climate Model (RCA3)*. Reports Meteorology

and Climatology 108, Swedish Meteorological and Hydrological Institute, SE-601 76 Norrköping, Sweden.

NERC 1975 *Flood Studies Report*. Volumes I–V. National Environmental Research Council, London, UK.

Olsson, J., Berggren, K., Olofsson, M. & Viklander, M. 2009 Applying climate model precipitation scenarios for urban hydrological assessment: a case study in Kalmar City, Sweden. *Atmos. Res.* **92**, 364–375.

Onof, C. & Arnbjerg-Nielsen, K. 2009 Quantification of anticipated future changes in high resolution design rainfall for urban areas. *Atmos. Res.* **92**, 350–363.

Rasch, P. J. & Kristjánsson, J. E. 1998 A comparison of the CCM3 model climate using diagnosed and predicted condensate parameterizations. *J. Climate* **11**, 1587–1614.

Semadeni-Davies, A., Hernebring, C., Svensson, G. & Gustafsson, L.-G. 2008 The impacts of climate change and urbanisation on drainage in Helsingborg, Sweden: Suburban stormwater. *J. Hydrol.* **350**, 114–125.

Slingo, J. 1987 The development and verification of a cloud prediction scheme for the ECMWF model. *Quart. J. Roy. Meteor. Soc.* **113**, 899–928.

Svenskt Vatten 2004 *Publication P90 – dimensioning of common sewers*. Svenskt Vatten AB, Motala (in Swedish).

Willén, U., Crewell, S., Baltink, H. K. & Sievers, O. 2005 Assessing model predicted vertical cloud structure and cloud overlap with radar and lidar ceilometer observations for the Baltex Bridge Campaign of CLIWA-NET. *Atmos. Res.* **75**, 227–255.

Willén, U. 2008 *Preliminary use of CM-SAF cloud and radiation products for evaluation of regional climate simulations*. Reports Meteorology 131, Swedish Meteorological and Hydrological Institute, SE-601 76 Norrköping, Sweden.

First received 13 December 2010; accepted in revised form 11 April 2011. Available online 7 February 2012